Journal of Building Engineering 45 (2022) 103549

Contents lists available at ScienceDirect

Journal of Building Engineering

journal homepage: www.elsevier.com/locate/jobe

Experimental study and prediction model of a liquid desiccant unit for humidification during the heating season

Hansol Lim [a], Soo-Jin Lee [b], Yuehong Su [a], Jae-Weon Jeong [b,*]

[a] Department of Architecture and Built Environment, University of Nottingham, University Park, Nottingham, NG7 2RD, UK
[b] Department of Architectural Engineering, College of Engineering, Hanyang University, Seoul, 04763, Republic of Korea

ARTICLE INFO

Keywords:
Liquid desiccant system
Humidification
Heating season
Empirical model
Response surface method

ABSTRACT

Liquid-desiccant-assisted air conditioning systems have attracted considerable interest owing to their potential to save energy and enhance performance through decoupled control of latent and sensible loads. In addition, several studies have suggested using the regenerator of a liquid desiccant system for humidification during the heating season; however, its performance under the winter weather condition has not yet been established. Therefore, the goal of this study is to develop the prediction models of the humidification performance of liquid desiccant systems during the heating season. Experiments were conducted to collect performance data based on the factorial experimental design method. Using the response surface method, two empirical models for the effectiveness of regeneration (R^2 = 0.927) and enthalpy exchange (R^2 = 0.934) were developed and experimentally validated under the actual conditions during the heating season within 10% error bounds. Significant parameters included the liquid-to-gas ratio and desiccant solution concentration and temperature. Moreover, the prediction model of the Sherwood number was developed which can be used for the numerical simulation. Additionally, the suitable operation settings of the regenerator for humidification were investigated to obtain higher energy and exergy efficiencies based on the developed prediction models. From the results, a higher liquid-to-gas ratio and lower concentration and temperature of the desiccant solution could be recommended considering both energy and energy efficiencies and the practical application of liquid desiccant systems.

1. Introduction

The concept of nearly- or net-zero-energy buildings is attracting increasing attention to reduce energy consumption and carbon emissions against climate change [1]. In South Korea, new public buildings over 1000 m^2 should be built as nearly-zero-energy buildings (nZEBs), and this requirement will be applied to almost all buildings from 2030 [2]. Similarly, the energy performance of buildings directive of the European Commission states that all new buildings must be nZEBs by 2021 [3].

To achieve nZEBs, energy saving for ventilation and air conditioning is essential in buildings, which is predicted to become the predominant factor of energy demand by 2050 [4]. In addition, the insulation and air tightness of nZEBs should be improved to prevent heat loss from the space [5] however, there is no way to reduce the latent load passively. Therefore, the latent load fraction is increased [6], and thus it is important to use a decoupled system for efficient dehumidification.

Liquid desiccant (LD)-assisted air conditioning systems are gaining popularity owing to their high potential for energy saving via decoupling of the handling of sensible and latent heat [7]. The absorber requires a relatively higher temperature of the cooling source compared with the conventional cooling coils, and a heating source is necessary for the regeneration process [8]. Hence, a heat pump is a good solution for providing simultaneous cooling and heating sources to the LD system, and various types of heat-pump-assisted LDs (HPLDs) have been suggested in previous studies [9,10].

Vapor compression heat pumps using compressors are the most popular owing to their compact size and high efficiency. Zhang et al. [9] suggested improving the performance of HPLD using additional heat removal devices at the condenser. A type of water-cooled HPLD demonstrated the best coefficient of performance (COP) values of 6.0 and 6.2 for systems in Beijing and Shanghai, respectively. In addition, a counter-flow-type HPLD has been proposed to improve the heat and mass transfer at the LD unit [10]. The performance of the proposed system was investigated experimentally, and a simulation model was built to optimize the performance. From the optimization, the number of mass transfer units and matching of the energy balance in the condenser

* Corresponding author.
E-mail address: jjwarc@hanyang.ac.kr (J.-W. Jeong).

https://doi.org/10.1016/j.jobe.2021.103549
Received 13 July 2021; Received in revised form 24 August 2021; Accepted 7 September 2021
Available online 2 November 2021

Nomenclature

b_x	Fixed error
COP	Coefficient of performance [−]
C_p	Specific heat [kJ/kg•°C]
Δp_{fan}	Pressure drop of the fan [Pa]
Ex	Exergy [kJ]
F	Face velocity [m/s]
g	Acceleration of gravity [m/s^2]
h	Enthalpy [kJ/kg]
H	Head loss [m]
$h_{a,\,eq}$	Equivalent enthalpy of solution [kJ/kg]
Le	Lewis number [−]
L/G	Liquid-to-gas ratio [−]
M	Mean value
$\dot{m}$	Mass flow rate [kg/s]
$\dot{m}_{hum}$	Humidification rate [kg/s]
NTU_m	Number of mass transfer units [−]
P	Power consumption [kW]
P_{atm}	Atmospheric pressure [kPa]
P_s	Vapor pressure of desiccant solution [kPa]
p_y	Random error
$\dot{Q}_{hum}$	Capacity of regenerator for latent load [kW]
Re	Reynolds number
RH	Relative humidity [%]
Sc	Schmidt number [−]
Sh	Sherwood number [−]
T	Temperature [°C]
S_r	Standard deviation
U_y	Overall uncertainty value
V	Volume of honeycomb media [m^3]
$\dot{V}$	Volume flow rate [m^3/s]

Greek Symbols

α_s	Specific surface area [m^2]
χ	Concentration [−]
ε	Effectiveness [−]
η	Efficiency [−]
λ_T	Vaporization latent heat at temperature T [kJ/kg]
ω	Humidity ratio [kg/kg$_a$]
ω_{eq}	Equilibrium humidity ratio [kg/kg$_a$]
φ	Latent heat of vaporization [kJ/kg]

Subscripts

a	Air
des	Designed value
ent	Enthalpy exchange
Ex	Exergy
i	Inlet
o	Outlet
r	Reference environment
reg	Regeneration
s	Desiccant solution

and evaporator had significant effects on the COP of the system. Meanwhile, the solid-state heat pump of the thermoelectric module (TEM) has been applied to the LD unit as a solid-state heat pump [11]. The energy-saving potential of the TEM-integrated LD unit was investigated through a detailed energy simulation, and the results showed that the efficiency of the TEM should be 1.7 times more than that of the current stage to achieve energy savings.

The focus of the HPLD system is mainly on dehumidification in the cooling season; however, it is necessary to consider the operation mode during the heating season. In the simple operation mode without additional devices, the heat pump is operated in the reverse cycle and the regenerator is used for heating and humidification purposes.

Su et al. [12] proposed the use of membrane-based LD dehumidification and humidification with an air source heat pump. From the performance analysis, air humidification was possible when the temperature and relative humidity of ambient air were above 0 °C and 70%, respectively. Lee et al. [13] investigated a suitable sump design for a desiccant solution in the HPLD unit, and the humidification operation using a regenerator during winter was included based on the reverse cycle of the heat pump. The results revealed that the separated sump for the absorber and regenerator can enhance the system COP by 37.5% and 4.95% in summer and winter, respectively. In addition, operation of the HPLD and evaporative cooling-assisted air conditioning system during winter was suggested to improve its performance [14]. Therefore, 42% of the operational energy can be saved by using a regenerator for heating and humidification.

As described above, there have been attempts to use a regenerator for heating and humidification during the heating season; however, no study has systematically assessed the humidification performance of regenerator under winter conditions. Although mathematical [15,16], empirical [17–20], computational fluid dynamic [21,22] and hybrid [23] models have been developed to predict the regeneration performance of LD systems, they only included the regeneration of the desiccant solution in the cooling season, or too complex to be simply used for designing or evaluating the humidification performance of LD system during the heating season. Therefore, it definitely necessary to develop the simple prediction model for humidification performance of LD system in the heating season. Thereby the LD system can be used not only for cooling season but in the heating season on the purpose of humidification. Moreover, the importance of humidification in the heating season is being increased as it was revealed that the high humidity reduces the spread of infectious disease such as COVID-19 [24,25].

Consequently, this study aims to investigate the characteristics of humidification performance during the heating season using a regenerator for heating and humidification applications. A series of experiments is conducted based on the factorial experimental design method. From the collected data, empirical models are developed to predict humidification performance during the heating season. Using the developed models, suitable operation settings are discussed herein considering the energy and exergy efficiencies.

2. Experimental methods

2.1. Regenerator overview

The purpose of the regenerator in an LD system is to regenerate the diluted desiccant solution for stable performance of dehumidification at the absorber during the cooling season. However, this study aims to use the regenerator to humidify the process air during the heating season without an absorber. When it is used for air conditioning system, the increased concentration of desiccant solution at the regenerator can be easily diluted by adding the water at the sump of regenerator to keep the constant concentration.

At the regenerator, the diluted desiccant solution directly meets the intake air for regeneration and exchanges moisture and heat. Therefore, moisture moves to the air from the diluted desiccant solution based on the partial vapor pressure difference between the desiccant solution and air. Hence, the partial vapor pressure of the desiccant solution (P_s) should be higher than that of the air side for regeneration. P_s depends on the temperature and concentration (Eq. (1)), exhibiting a higher value

with a higher temperature and lower concentration of the desiccant solution [8].

In previous studies [17,18], the humidification performance was defined using the regeneration effectiveness (ε_{reg}) in Eq. (2). The equilibrium humidity ratio (ω_{eq}) in Eq. (3) constitutes P_s and the atmospheric pressure (P_{atm}). Therefore, a higher temperature with a lower concentration of the desiccant solution yields a higher value of ω_{eq}. In addition, if the partial vapor pressure of air (P_a) is fixed, the humidification rate ($\dot{m}_{hum}$) in Eq. (4) would be greater with higher P_s.

$$P_s = f(T_s, \chi_s) \tag{1}$$

$$\varepsilon_{reg} = \frac{\omega_{a,\,o} - \omega_{a,\,i}}{\omega_{eq} - \omega_{a,\,i}} \tag{2}$$

$$\omega_{eq} = 0.622 \frac{P_s}{(P_{atm} - P_s)} \tag{3}$$

$$\dot{m}_{hum} = \dot{m}_a(\omega_{a,\,o} - \omega_{a,\,i}) \tag{4}$$

During the regeneration process, the enthalpy of the process air increases through the exchange of heat and moisture from the desiccant solution (i.e., enthalpy exchange). Therefore, it can be defined using the enthalpy exchange effectiveness (ε_{ent}) consisting of the equivalent enthalpy of the solution ($h_{a,\,eq}$), as in Eqs. (5) and (6), respectively.

$$h_{a,\,eq} = 1.006T_{s,\,i} + \omega_{eq}2501 + 1.86T_{s,\,i} \tag{5}$$

$$\varepsilon_{ent} = \frac{h_{a,\,o} - h_{a,\,i}}{h_{a,\,eq} - h_{a,\,i}} \tag{6}$$

In this study, the humidification using only desiccant solution was considered, although the hot water has a higher partial water vapor than that of desiccant solution. It was because the purpose of using regenerator as a humidifier is to use LD system all the year over, and it is difficult to totally change the desiccant solution sump to the water sump when the heating season is started in the aspect of management. In addition, the freezing problem may concern at the downstream of honeycomb media if the water is directly used for humidification in winter.

2.2. Test configurations

The design of the LD unit for the experiment was based on the HPLD and evaporative cooling-assisted air conditioning system, HPLD-IDECOAS, from the previous studies [26,27]. A cross-flow type structure with honeycomb media (CELdek 7090-15) [28] was used to construct the regenerator, as shown in Fig. 1. The size of the packing media was 350 mm (width) × 350 mm (height) × 700 mm (length) and its specific surface area (α_s) was 360 m^2/m^3. In addition, we used an

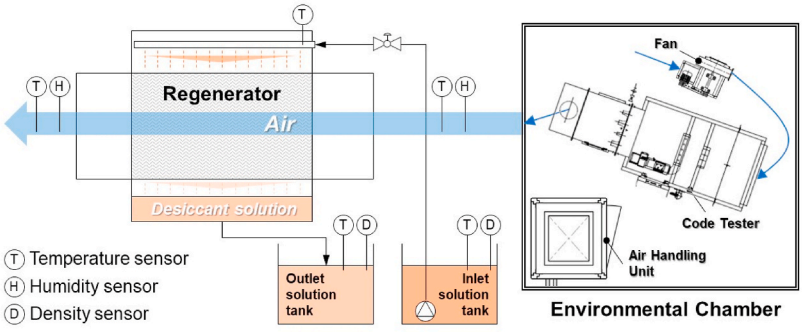

(a) Sensor positions and equipment arrangements

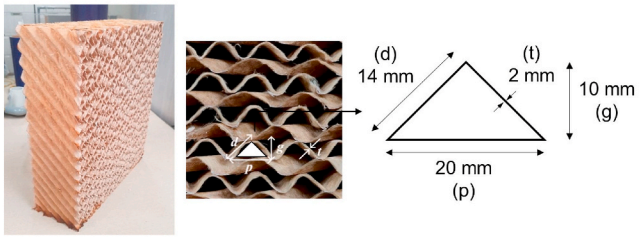

(b) Honeycomb media (CELdek 7090-15)

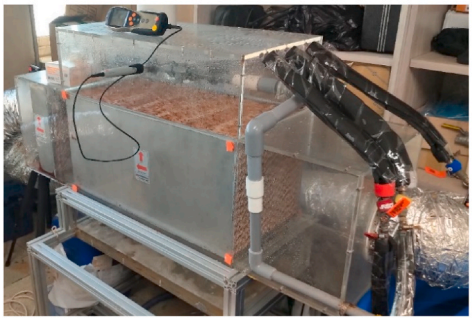

(c) Cross-flow type regenerator

(d) Environmental chamber

Fig. 1. Experimental setup.

aqueous lithium chloride (LiCl) desiccant solution with a concentration between 20% and 30% for humidification during the heating season. Two storage tanks were used for the inlet and outlet desiccant solutions. The experimental unit was designed as an open loop for the stable condition of the inlet desiccant solution (i.e., weak desiccant solution), and submersible pumps (HYUBSHIN, UP500) [29] were used to spray the desiccant solution onto the honeycomb media through a manifold and nozzles to sufficiently wet the media. We selected the mass flow rate of the desiccant solution as 0.105 kg/s (i.e., 5 L/min) considering the liquid-to-gas ratio (L/G), duration of each test operation, and maximum capacities of the fan and pump.

The inlet air to the regenerator was conditioned and supplied from the environmental chamber (Fig. 1c). The air volume flow rate can be controlled using a variable-speed fan, and its value was measured in real time using a code tester. The temperature of the desiccant solution was adjusted using an electric heating coil in the tank for a weak desiccant solution. All the test rig was validated in the previous study [18].

In Fig. 1a, the positions of the sensors are marked for the desiccant solution and air at the inlet and outlet of each process. The temperature and relative humidity of the inlet and outlet air were recorded within 10-s intervals using Testo 175H1 (temperature range of -20–55 °C with ± 0.4 °C accuracy, and relative humidity range of 0%–100% with ± 2% accuracy). The inlet temperature of the desiccant solution at the nozzle of the manifold was logged within 10-s intervals using a Testo 735-2 data logger and penetration probe (-50–275 °C with accuracy of ± 0.5 °C). In both solution tanks, the temperature and density of the desiccant solution were measured in order to derive the concentration of desiccant solution indirectly. In addition, the density and temperature of solution was measured intermittently because both values did not fluctuate significantly (particularly at the inlet solution tank). The density measurement was performed using a glass hydrometer with the range of 1000–1400 kg/m^3 and accuracy of 1 kg/m^3.

2.3. Design parameters

The design parameters for predicting the humidification performance were selected based on previous studies [17,18], including the air temperature (T_a), humidity ratio of air (ω_a), L/G, and temperature (T_s) and concentration (χ_s) of the desiccant solution. The dependent variables representing the humidification performance are the regeneration effectiveness (ε_{reg}) and enthalpy exchange effectiveness (ε_{ent}), given in Eqs. (2) and (6), respectively.

The outdoor air temperature during the heating season is lower than -15 °C according to the weather conditions of Seoul, Korea [30]; therefore, the freezing temperature of the desiccant solution should be less than -20 °C for operation under extremely cold weather. Hence, the concentration of the desiccant solution (χ_s) ranged from 20% to 30% to avoid freezing problems [31].

In a previous study [18], the solution temperature (T_s) generally ranged from 40 to 60 °C for workable regeneration in an LD system. Although a T_s value higher than 60 °C contributes to better regeneration performance, the energy required to heat the desiccant solution will be wasted, and over-humidification may occur. The L/G of the regeneration system ranged from 1 to 3 based on previous studies [18]. Similar to the solution temperature (T_s), a higher L/G yields better regeneration; however, more energy will be used for unnecessary humidification. Further details regarding the operating energy are discussed in Section 4.

The air conditions for the experiment were selected based on the outdoor air conditions during the heating season. As shown in Fig. 2, the outdoor air temperature (T_a) and humidity ratio (ω_a) in the heating season from November to March in Seoul, Korea, ranged from -15 to 20 °C and 0.004–0.01 kg/kg$_a$, respectively. However, there was a limitation on the cooling performance of the environment chamber for cooling air to lower than approximately 8 °C and drying air to approximately 0.004 kg/kg$_a$ under the experimental conditions. Hence, the air conditions inside the blue shaded area in Fig. 2 were considered for the designed experiments. Meanwhile, the air conditions outside the blue area represent the actual outdoor air during the heating season (Section 3.4). Consequently, Table 1 presents the range of the design parameters used to develop the empirical models for predicting the humidification performance.

2.4. Experimental design

Two dependent parameters were predicted: the regeneration effectiveness (ε_{reg}) in Eq. (2), and the enthalpy exchange effectiveness (ε_{ent}) in Eq. (6). Therefore, two empirical prediction models were derived from the same experimental datasets.

Table 1
Range of design parameters.

Design parameter	Low	High
L/G [−]	1	3
χ_s [−]	0.2	0.3
T_s [°C]	40	60
T_a [°C]	8	20
ω_a [kg/kg$_a$]	0.004	0.010

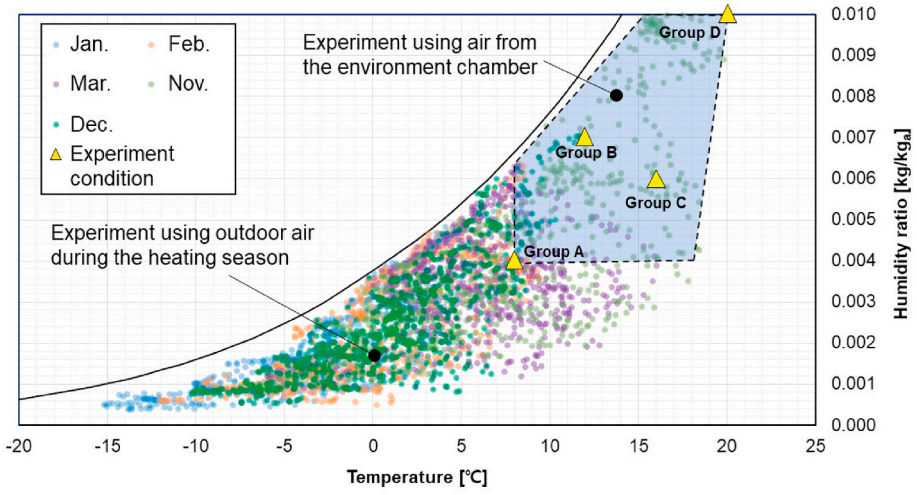

Fig. 2. Outdoor air conditions for the experiments.

To develop the models, the design of experiments (DOE) was used to first identify significant design parameters statistically, and then to apply the response surface method in Design Expert version 11 [32].

The 2^k factorial design method was used for the temperature (T_s) and concentration (χ_s) of the desiccant solution because they have a linear relationship with both regeneration effectiveness (ε_{reg}) and enthalpy exchange effectiveness (ε_{ent}) [17,18] within their range, as shown in Table 1. Whereas, the linear relationship between the L/G and dependent variables was uncertain. In the literature, the regeneration performance increased as the L/G increased; however, there may be a critical point at which the regeneration performance converges. For this reason, the 3^k factorial design method was used for the L/G by adding the median value (i.e., L/G = 2).

The factor arrangements using the DOE could not be applied to the air conditions. Although the air conditions include the ranges defined in Table 1, their combinations using the DOE do not produce meaningful values. For example, the combination of low air temperature (i.e., T_a = 8 °C) with a high humidity ratio (i.e., ω_a = 0.010 kg/kg$_a$) is over 100% relative humidity. Meanwhile, the combination of high air temperature (i.e., T_a = 20 °C) with a low humidity ratio (i.e., ω_a = 0.004 kg/kg$_a$) does not exist in the weather data. Therefore, the DOE was not used for the air conditions; instead, the representative combinations of air conditions were selected to cover the weather data inside the blue area in Fig. 2, which can be generated from the environment chamber. The four selected air conditions are highlighted by the yellow triangles and named as Group A to D in Fig. 2.

Finally, two levels for the temperature (T_s) and concentration (χ_s) of the desiccant solution, three levels for the L/G, and four air conditions provided a total of 48 experimental sets, as shown in Table A1.

2.5. Uncertainty analysis

For the analysis of uncertainty, the guidelines from ASHARE [33] were used in this study. The overall uncertainty value (U_y) incorporates the propagation of error (b_y) and random error (p_y), as in Eq. (7). The propagation of error (b_y) is the propagated uncertainty via a data reduction equation, which is the regeneration effectiveness, enthalpy effectiveness and the amount of humidification in this study. It was calculated using Eq. (8) based on the equations in Eqs. (2), (4) and (6). The fixed error (b_x) is from the error rate of the sensor itself, and p_y is from the randomness, which is defined in Eq. (9).

The calculated overall uncertainty values are listed in Table 2, which were continuously recorded over time. The uncertainty of the humidity was calculated using the relative humidity, which is an indicator used in the sensor. All measured averaged overall uncertainties demonstrate similar values with the fixed error. Thus, the values remained stable during the measurements without fluctuating.

$$U_y = \sqrt{\left(b_y{}^2 + p_y{}^2\right)} \tag{7}$$

$$b_y = \sqrt{\sum_{i=1}^{n}\left(\frac{dy}{dx_i}b_{x_i}\right)^2} \tag{8}$$

Table 2
Overall uncertainty of measured data.

	Average	Standard deviation
Ta, i [°C]	0.41	0.01
$RH_{a,i}$ [%]	2.12	0.18
Ta, o [°C]	0.41	0.02
$RH_{a,o}$ [%]	2.15	0.42
T_s [°C]	0.52	0.02
ε_{reg} [−]	0.036	0.013
ε_{ent} [−]	0.032	0.011
$\dot{m}_{hum}$ [g/kg$_a$]	0.46	0.06

$$p_y = \frac{2S_r}{\sqrt{M}} \tag{9}$$

3. Experimental and modelling results

3.1. Humidification performance of regenerator

Each experiment was performed for approximately 10 min; however, the initial data until 200 s were excluded because the recorded inlet solution temperature slowly increased before stabilizing. In Fig. 3, the operation data for experiment sets 3 and 34 is plotted to show the inlet desiccant solution temperature and the air condition at the inlet and outlet. The experiment sets 3 and 34 were selected because they showed the lowest and highest humidification performances for the driest air condition (i.e., T_a = 8 °C, ω_a = 0.004 kg/kg$_a$) among designed experiments.

In Fig. 3a and b, the air temperature increased to 30.4 °C as a result of heat exchange with the desiccant solution, whose inlet temperature was 40.6–43.2 °C. In addition, the inlet air humidity ratio increased to over 0.010 kg/kg$_a$ because of the transfer of water vapor from the desiccant solution. In this experiment set 3, the average regeneration effectiveness was 0.480±0.015, and the enthalpy exchange effectiveness was 0.651±0.021. In Fig. 3c and d, the process air is heated and humidified to 37.7 °C and 0.031 kg/kg$_a$ by the desiccant solution whose temperature was 59.8 °C–60.9 °C. In this experiment set 34, the average regeneration and enthalpy exchange effectiveness were 0.263±0.005 and 0.304±0.005, respectively.

The lowest recommended criterion for the relative humidity of room air is 30% [34], and that for room air temperature for thermal comfort is 20 °C [35]. Therefore, the humidity ratio of room air should be higher than 0.00434 kg/kg$_a$ during the heating season. Likewise, the humidity ratio of the process air must be higher than 0.00434 kg/kg$_a$, and the appropriate target humidity ratio can be determined according to the volume flow rate of air.

The humidity ratio of the humidified process air was 0.008–0.059 kg/kg$_a$ in all 48 experimental cases, indicating that the humidification performance of the regenerator is sufficient to humidify a room during the heating season. Moreover, the outlet air temperature was 23.9–48.1 °C in all cases; therefore, part of the sensible load can be accommodated and heat loss from the ventilation can be reduced by using the regenerator for humidification during the heating season.

3.2. Effects of design parameters on the humidification performance

To investigate the effects of the design parameters on the regeneration and enthalpy exchange effectiveness values, a parametric analysis was conducted as shown in Fig. 4. In addition, the effects of the design parameters on the amount of humidification were analyzed to investigate the humidification capacity of the regenerator in the LD unit. Owing to many variables affecting on the humidification performances which may cause confusion, the experiment cases in Table A1 and air condition groups in Fig. 2 are sorted by color mark and labels in each figure. Furthermore, Pearson's correlation analysis was also conducted to statistically quantify the effects between the design parameters and humidification performances (Table 3).

The enthalpy exchange effectiveness is always slightly higher than the regeneration effectiveness, and both are highly correlated (R = 0.977, p-value < 0.01). This is natural because the enthalpy exchange includes both mass transfer and heat transfer, and the regeneration effectiveness is directly related to the mass transfer between air and the LD. In addition, the L/G significantly positively correlates with the humidification performance (Fig. 4a). However, a negative correlation was observed between the humidification performance and inlet solution temperature (T_s), as shown in Fig. 4c. Meanwhile, other design parameters (i.e., T_a, ω_a, and χ_s) exhibit weak correlations with the

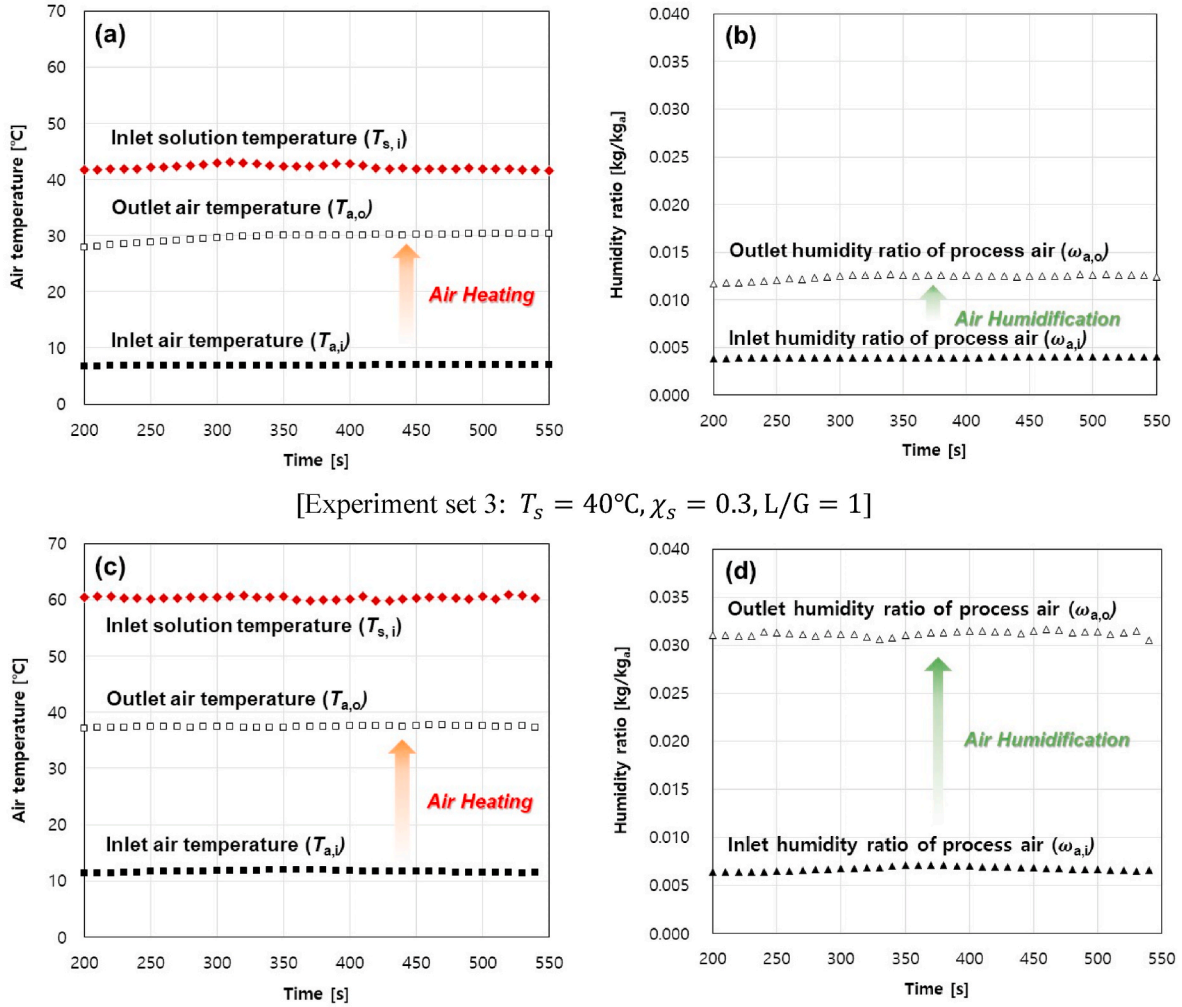

Fig. 3. Example of regenerator performance for the humidification (χ_s = 0.3, L/G = 3).

humidification performance (Fig. 4e, g, and 4i, and Table 3).

The amount of humidification positively correlates with both the L/G and T_s (Fig. 4b and d), with Pearson's values of 0.347 and 0.753, respectively. In addition, there are very weak or insignificant correlations between the amount of humidification and outdoor air conditions (T_a and ω_a), as shown in Fig. 4f and h and Table 3. Contrary to the results of the humidification performance, the amount of humidification has a strong negative correlation with the concentration (R = -0.367, p-value < 0.01), as shown in Fig. 4j. The results between the humidification performance and the amount of humidification differ because the effectiveness parameters are ratios, as defined in Eqs. (2) and (6), respectively.

3.3. Simplified effectiveness models of regenerator for humidification

The response surface method was used to develop empirical models. There were two predicted parameters, namely: regeneration effectiveness (ε_{reg}) and enthalpy exchange effectiveness (ε_{ent}). A further three parameters were selected for modeling from the parametric and correlation analysis of the design parameters in Section 3.2: the L/G, solution temperature (T_s), and concentration of desiccant solution (χ_s).

The 1506 data samples collected from the 48 experimental sets were used for statistical modeling. In the response surface method, the quadratic model exhibited the best fit in both developed models, with R^2 values of 0.927 and 0.934 for ε_{reg} and ε_{ent}, respectively.

For statistical validation, ANOVA was conducted, and the results showed that all independent variables for the two developed prediction models produced p-values lower than 0.05, as determined by the F-test (Table 4). In addition, the L/G demonstrated the highest effect sizes of 0.6882 and 0.6370 for ε_{reg} and ε_{ent}. Moreover, the effect sizes of the desiccant solution temperature (T_s) were the second highest among the independent variables. Similar to the correlation analysis results in Section 3.2, the concentration of the desiccant solution (χ_s) has a small effect size on ε_{reg} and ε_{ent}; however, it was included in the models to improve the prediction accuracy.

The normal plots of residuals were established to validate the normal distribution of the collected data, as in Fig. 5, and the residuals were verified to properly follow the normal distribution. The resulting simplified empirical models for humidification performance are provided in Eqs. (10) and (11), and their coefficients are listed in Table 5. A comparison between the predicted and actual values from the experiments is presented in Fig. 6.

$$\varepsilon_{reg} = \alpha_0 + \alpha_1\chi_s + \alpha_2 T_s + \alpha_3 L/G + \alpha_4\chi_s T_s + \alpha_5\chi_s L/G + \alpha_6 T_s L/G + \alpha_7{\chi_s}^2 + \alpha_8{T_s}^2 + \alpha_9 L/G^2 \quad (10)$$

$$\varepsilon_{ent} = \beta_0 + \beta_1\chi_s + \beta_2 T_s + \beta_3 L/G + \beta_4\chi_s T_s + \beta_5\chi_s L/G + \beta_6 T_s L/G + \beta_7{T_s}^2 + \beta_8 L./G^2 \quad (11)$$

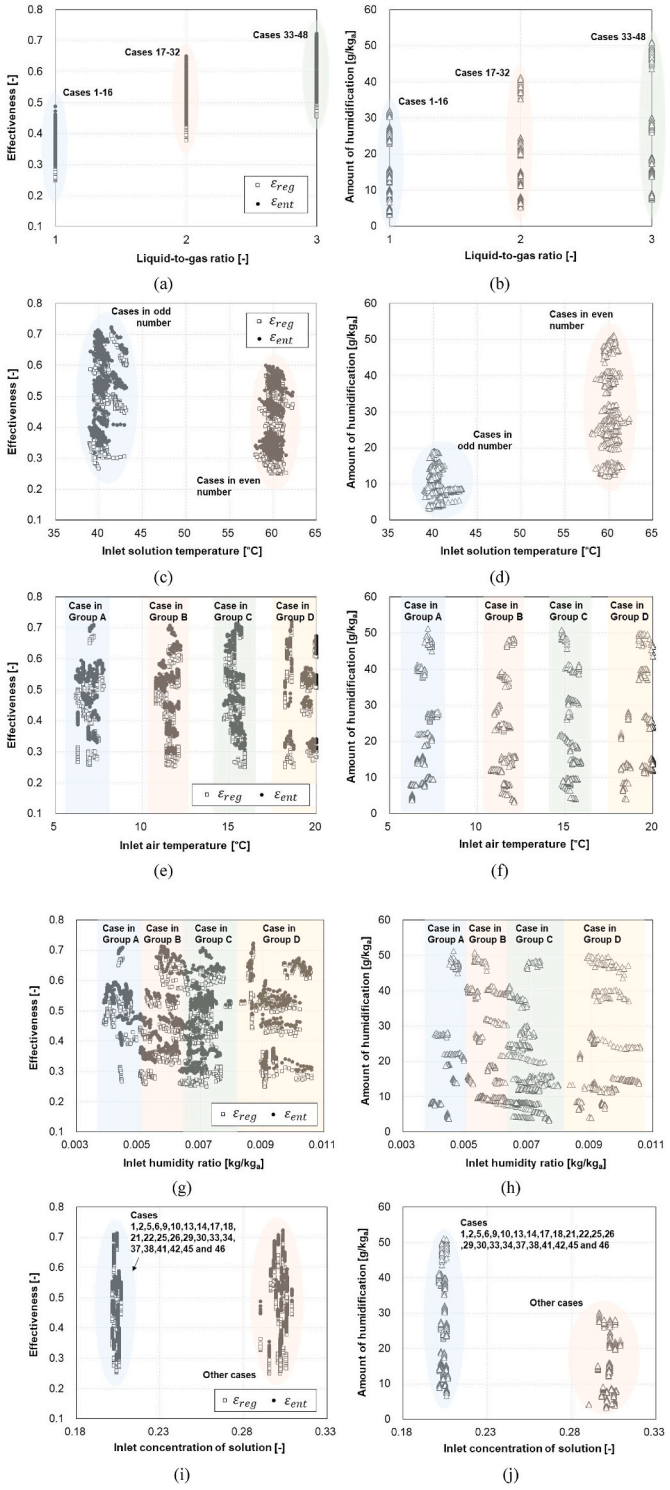

Fig. 4. Effects of design parameters on the humidification performance (Cases and Group can be checked in Fig. 2 and Table A1).

3.4. Validation of the developed models

Additional experiments were conducted to investigate and validate the developed models under the actual operation situation since there was no other experimental data in literatures to validate the developed models. Conditioned air from the environmental chamber exhibited the lowest temperature of 6.2 °C; therefore, the validation experiments used the outdoor air of Seoul, Korea, in the period from December 16, 2019, to February 6, 2020. The target outdoor air temperature was -10 – 5 °C, and was separated into three groups for methodical experiments. There were 24 experimental sets for validation, as shown in Table A2. The medium value of the L/G was excluded in designing the validation experiments because its linearity had already been revealed, as in Section 3.2.

A total of 1044 data points were collected from the validation experimental sets. The predicted humidification performance showed good agreement with the actual values in the validation experiments within 10% of the root mean square error (RMSE) bounds (Fig. 7). Therefore, the developed models for humidification performance can be used under outdoor air conditions in the heating season below 20 °C.

Table 3
Pearson's correlation coefficients between design parameters and performance parameters.

	L/G	T_s	χ_s	T_a	ω_a
ε_{reg}	0.898**	-0.342**	-0.054*	0.082**	-0.015
ε_{ent}	0.890**	-0.372**	0.090**	-0.041	-0.102**
$\dot{m}_{hum}$	0.347**	0.753**	-0.367**	-0.021	-0.063*

**Correlation is significant at the 0.01 level *Correlation is significant at the 0.05 level

Table 4
ANOVA results of the developed empirical models.

(a) Regeneration effectiveness

Source	Sum of squares	*df*	Mean square	*F*-value	*p*-value	Effect size
Model	19.584	9	2.2	2105	0.0000	
A: χ_s	0.023	1	0.0	22	0.0000	0.0011
B: T_s	1.167	1	1.2	1129	0.0000	0.0552
C: L/G	14.543	1	14.5	14,071	0.0000	0.6882
AB	0.024	1	0.0	23	0.0000	0.0011
AC	0.004	1	0.0	4	0.0493	0.0002
BC	0.159	1	0.2	153	0.0000	0.0075
A^2	0.017	1	0.0	17	0.0000	0.0008
B^2	0.026	1	0.0	26	0.0000	0.0012
C^2	0.145	1	0.1	141	0.0000	0.0069
Residual	1.547	1497	0.0			
Corrected total	21.131	1506				

(b) Enthalpy exchange effectiveness

Source	Sum of squares	*df*	Mean square	*F*-value	*p*-value	Effect size
Model	17.261	8	2.2	2663	0.0000	
A: χ_s	0.109	1	0.1	135	0.0000	0.0059
B: T_s	1.604	1	1.6	1980	0.0000	0.0868
C: L/G	11.769	1	11.8	14,526	0.0000	0.6370
AB	0.005	1	0.0	6	0.0122	0.0003
AC	0.073	1	0.1	90	0.0000	0.0039
BC	0.071	1	0.1	87	0.0000	0.0038
B^2	0.019	1	0.0	23	0.0000	0.0010
C^2	0.205	1	0.2	253	0.0000	0.0111
Residual	1.214	1498	0.0			
Corrected total	18.475	1506				

3.5. Dimensionless model for numerical simulation

The simplified model developed in Section 3.3 is suitable for quick evaluation of the humidification performance, such as for annual performance simulation. However, these models are based on the data from the test rig in Section 2, and it may derive unexpected results with the regenerator that has different specifications. Therefore, the Sherwood number (*Sh*) model in Eq. (12) was established in the form of *Sh* correlation that was arranged into pertinent dimensionless groups using the Buckingham π theory [36–39]. The constant coefficients for Eq. (12) were derived by nonlinear regression of the experimental data from

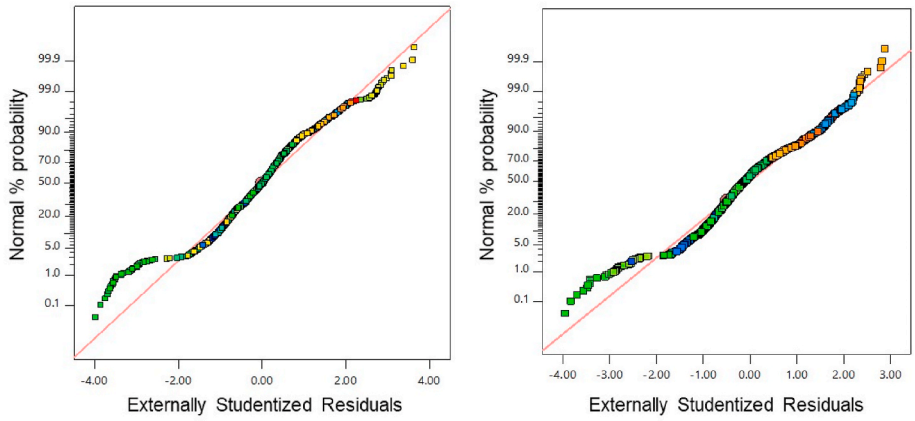

(a) Regeneration effectiveness (b) Enthalpy exchange effectiveness

Fig. 5. Normal plots of residuals.

Table 5
Model coefficients.

(a) Regeneration effectiveness				
α_0	α_1	α_2	α_3	α_4
2.146224	-8.408653	-0.039957	0.291520	0.009424
α_5	α_6	α_7	α_8	α_9
-0.043581	-0.001327	15.485866	0.000364	-0.021169
(b) Enthalpy exchange effectiveness				
β_0	β_1	β_2	β_3	β_4
0.831601	0.779026	-0.031575	0.307107	-0.004320
β_5	β_6	β_7	β_8	
-0.185758	-0.000885	0.000302	-0.024933	

Table A1 and A2.

$$Sh = 5.12 \times 10^{-4} Re_a^{1.363}\, Sc_a^{0.333}\, LG^{0.91}\, (1-\chi_s)^{1.51} \quad (12)$$

Consequently, with the Sherwood number, the humidification performance can be numerically simulated based on the method in the previous studies [18,39]. The detail for numerical simulation is described in Appendix B. The comparison results are in Fig. 8 within 12% of the RMSE. Therefore, the humidification performance during the heating season can be evaluated using the proposed model and numerical simulation method under various regenerator.

4. Discussion

In this section, the operation of the regenerator is discussed for humidification during the heating season. An energy simulation was conducted based on the developed prediction models for the regeneration and theoretical models.

4.1. Simulation overview

The purpose of using a regenerator during the heating season is to humidify and heat the process air. Therefore, it was assumed that the regenerator aims to accommodate the latent load in the heating season, and a binary control was selected for operating the regenerator [14].

The designed outdoor air conditions for the heating season included the temperature of -11.3 °C and relative humidity of 63% (0.0009 kg/kg$_a$) based on the TAC 2.5% [40]. In addition, the supply air flow rate was set to 120 m^3/h based on the maximum ventilation flow rate of an 84-m^2 apartment in Korea [41]. The input variables comprised the operational parameters of the regenerator, specifically: the L/G, and temperature (T_s) and concentration (χ_s) of the desiccant solution within valid ranges of the developed models.

4.2. Effects of operational parameters on the energy efficiency

To estimate the energy efficiency, the COP for humidification (Eq.

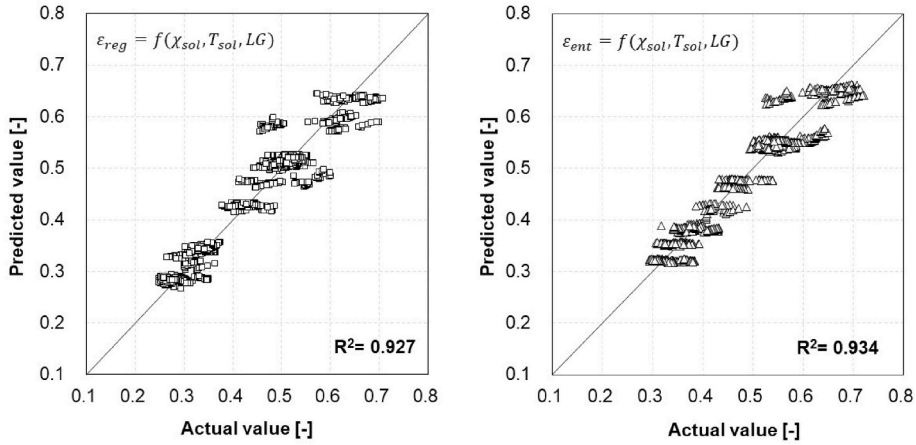

(a) Regeneration effectiveness (b) Enthalpy exchange effectiveness

Fig. 6. Comparison results between predicted and measured values for the two developed models.

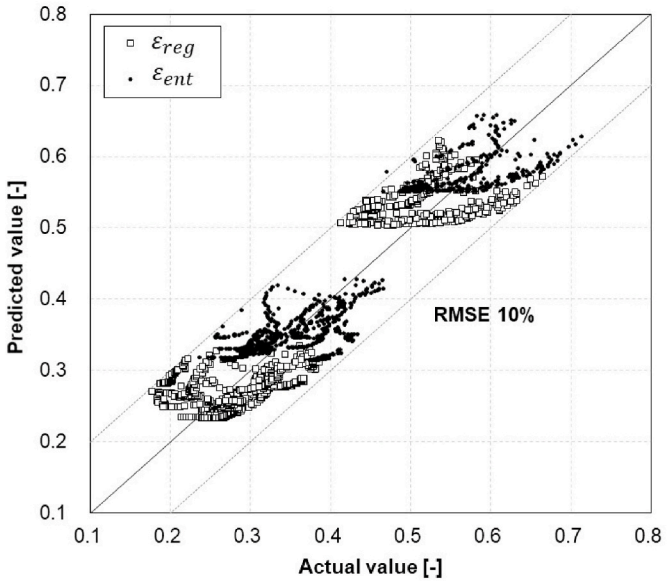

Fig. 7. Validation results from additional experimental data.

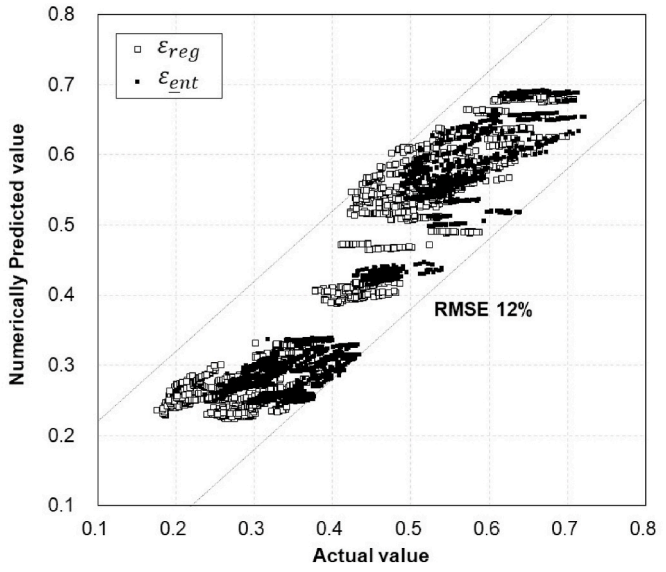

Fig. 8. Comparison results between predicted and measured values for the numerical simulation.

(13)) was derived according to the operational parameters. The energy efficiency for the latent load is the focus of this study; therefore, we only used the capacity of the regenerator for the latent load ($\dot{Q}_{hum}$) to calculate the COP for humidification, as defined in Eq. (14). In addition, the power consumption of the regenerator was obtained using those of the electric heating coil, pump, and fan, as in Eq. (15). The equipment for heating the desiccant solution could be more energy efficient; however, an electric heating coil was used for this investigation.

$$COP = \frac{\dot{Q}_{hum}}{P_{tot}} \tag{13}$$

$$\dot{Q}_{hum} = \dot{m}_a \varphi \left(\omega_{a,\,o} - \omega_{a,i}\right) \tag{14}$$

$$P_{tot} = P_{heating} + P_{fan} + P_{pump} \tag{15}$$

According to the three operational parameters, the effectiveness values of regeneration and enthalpy exchange were determined using Eqs. (10) and (11), respectively. Then, the outlet humidity ratio and enthalpy of the process air could be calculated using Eqs. (16) and (17), which are the transpose formulae of Eqs. (2) and (6), respectively. The partial vapor pressure of the desiccant solution (P_s), in Eqs. (1) and (3), is a property of LiCl, and was derived using the Engineering Equation Solver program in this study.

Additionally, the outlet temperature can be calculated from the outlet enthalpy and humidity ratio of the process air. The enthalpy difference between the inlet and outlet air is assumed to be the same as that between the inlet and outlet desiccant solutions based on the law of conservation of energy. The difference between the inlet and outlet concentrations of the desiccant solution was negligible owing to their magnitudes, and the inlet concentration of the desiccant solution was assumed to be constant by adding tap water to the sump. Therefore, the outlet temperature of the desiccant solution could be calculated using the concentration and enthalpy of the desiccant solution based on the properties of LiCl.

$$\omega_{a,o} = \varepsilon_{reg}\left(\omega_{eq} - \omega_{a,\,i}\right) + \omega_{a,\,i} \tag{16}$$

$$h_{a,\,o} = \varepsilon_{ent}\left(h_{a,\,eq} - h_{a,\,i}\right) + h_{a,\,i} \tag{17}$$

The power consumption was calculated based on the theoretical models for the electric heating coil ($P_{heating}$), fan (P_{fan}), and pump (P_{pump}) in Eqs. 18–21 [42]. The efficiencies of the fan (η_{fan}) and pump (η_{pump}) were assumed as 0.5 and 0.6, respectively, which are general values on the commercial market. The volume flow rate of the fan ($\dot{V}_a$) remained constant, and the mass flow rate of the pump ($\dot{m}_s$) varied according to the L/G. The designed power consumption of the pump ($P_{pump,\,des}$) was calculated using Eq. (20) for the designed mass flow rate of the pump ($\dot{m}_{s,\,des}$). Then, the actual power consumption of the pump (P_{pump}) could be derived based on the affinity law in Eq. (21). The pressure drop (Δp_{fan}) and head loss (H) of the LD system were set to be 75 Pa and 0.4 m, respectively [43,44].

$$P_{heating} = \dot{Q}_{heating} = \dot{m}_s C_{p,s}\left(T_{s,\,i} - T_{s,\,o}\right) \tag{18}$$

$$P_{fan} = \frac{\dot{V}_a \Delta p_{fan}}{\eta_{fan}} \tag{19}$$

$$P_{pump,\,des} = \frac{\dot{m}_{s,\,des} \times H \times g}{\eta_{pump}} \tag{20}$$

$$P_{pump} = P_{pump,\,des} \times \left(\frac{\dot{m}_s}{\dot{m}_{s,\,des}}\right)^3 \tag{21}$$

The simulation results for the COP for humidification are shown in Fig. 9, according to the three operational parameters. Consequently, a high L/G, and low concentration and high temperature of the desiccant solution demonstrated a high COP in the range of 0.35–0.71. Statistical analysis was conducted to investigate the effects of each parameter on the COP via correlation analysis. The resulting Pearson's coefficients were -0.737, -0.581, and 0.295 for the concentration (χ_s) and temperature (T_s) of the desiccant solution, and L/G, respectively. Here, χ_s has the highest value because it does not require energy to control. Therefore, it is reasonable to use a low χ_s value during the heating season to reduce the energy required for humidification. In addition, the difference between the minimum and maximum COP values varied from 0.11 to 0.20, according to the solution temperature (T_s) between 40 and 60 °C. However, the L/G had a relatively small effect on the COP for humidification.

4.3. Effects of operational parameters on the exergy efficiency

This section aims to search for suitable operation settings for achieving a high exergy efficiency. The exergy efficiency indicates how

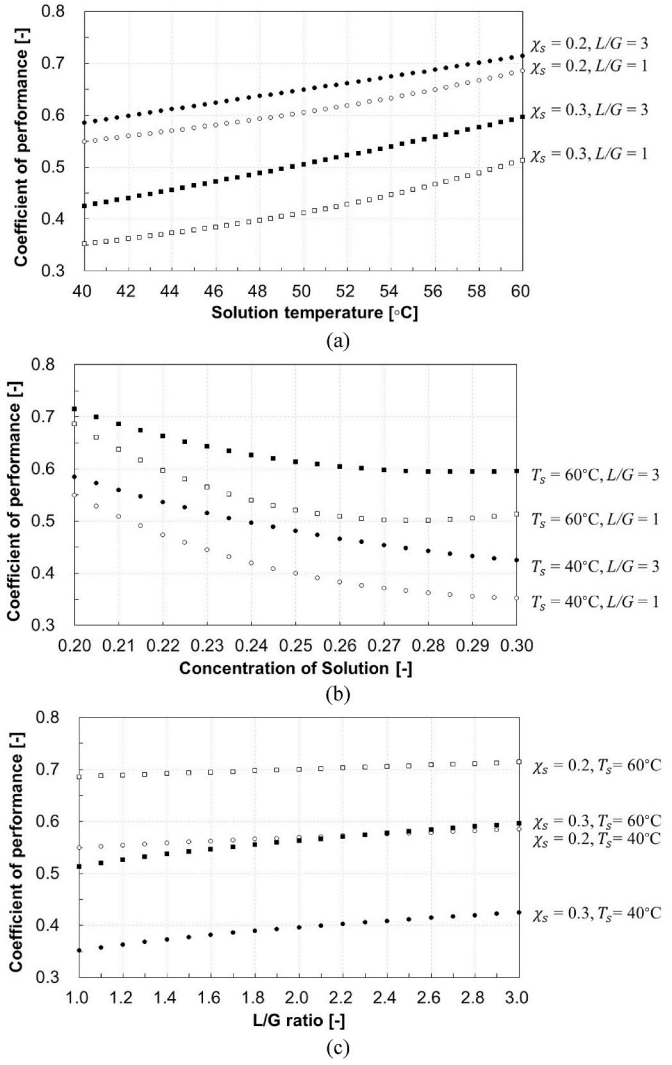

Fig. 9. Effects of operational parameters on the coefficient of performance during the humidification process.

the system effectively uses its maximum available energy during a reversible reaction. A high exergy efficiency reflects high energy quality in the system, hence the system is more sustainable regarding energy losses and internal irreversible reactions [45].

The exergy efficiency (η_{Ex}) can be derived using Eqs. 22–26, taken from a previous study [46]. The conditions of the reference environment were assumed to be 20 °C and 30% relative humidity (ω_r = 0.00434 kg/kg$_a$) for the exergy analysis, which are the recommended room conditions during the heating season [34,35]. Other factors for the analysis were the same as those provided in Section 4.2.

$$Ex_{a,\,i} = T_r \dot{m}_a \left(C_{p,a} \ln\left(\frac{T_{a,\,i}}{T_r}\right) + \varphi\left(\frac{\omega_{a,\,i} - \omega_r}{T_a^*}\right)\right) \tag{22}$$

$$Ex_{a,\,o} = T_r \dot{m}_a \left(C_{p,a} \ln\left(\frac{T_{a,\,o}}{T_r}\right) + \varphi\left(\frac{\omega_{a,\,o} - \omega_r}{T_a^*}\right)\right) \tag{23}$$

$$Ex_{s,i} = T_r \dot{m}_s \left(C_{p,s} \ln\left(\frac{T_{s,i}}{T_r}\right) + \varphi\left(\frac{\omega_{eq,i} - \omega_r}{T_s^*}\right)\right) \tag{24}$$

$$Ex_{s,o} = T_r \dot{m}_s \left(C_{p,s} \ln\left(\frac{T_{s,o}}{T_r}\right) + \varphi\left(\frac{\omega_{eq,o} - \omega_r}{T_s^*}\right)\right) \tag{25}$$

$$\eta_{Ex} = 1 - \frac{\left(Ex_{a,\,i} + Ex_{s,\,i}\right) - \left(Ex_{a,o} + Ex_{s,o}\right)}{\left(Ex_{a,\,i} + Ex_{s,\,i}\right)} \tag{26}$$

In Fig. 10, the exergy efficiency results are displayed according to the three operational parameters of the regenerator. Consequently, higher χ_s and L/G values generated high exergy efficiencies (η_{Ex}) in all cases. Lower solution temperatures (T_s) generally exhibited high η_{Ex}, and optimal T_s values were realized according to the L/G.

Regarding the L/G, the available amount for humidification and enthalpy exchange (i.e., heat and mass transfer) increased as the mass flow rate of the desiccant solution ($\dot{m}_s$) increased, and the effectiveness of the humidification performance increased. The reason for the increase in η_{Ex} is that the increase rate of effectiveness was higher than that of exergy for humidification and enthalpy exchange.

Meanwhile, in the case of the concentration of the desiccant solution (χ_s), the exergy for humidification and enthalpy exchange and the effectiveness of the humidification performance decreased as the partial vapor pressure difference between the desiccant solution and process air decreased with increasing concentration. However, η_{Ex} increased because the decrease in the humidification performance was less than the exergy decrease.

According to the increase in the desiccant solution temperature (T_s), the exergy of humidification and enthalpy exchange increased as the

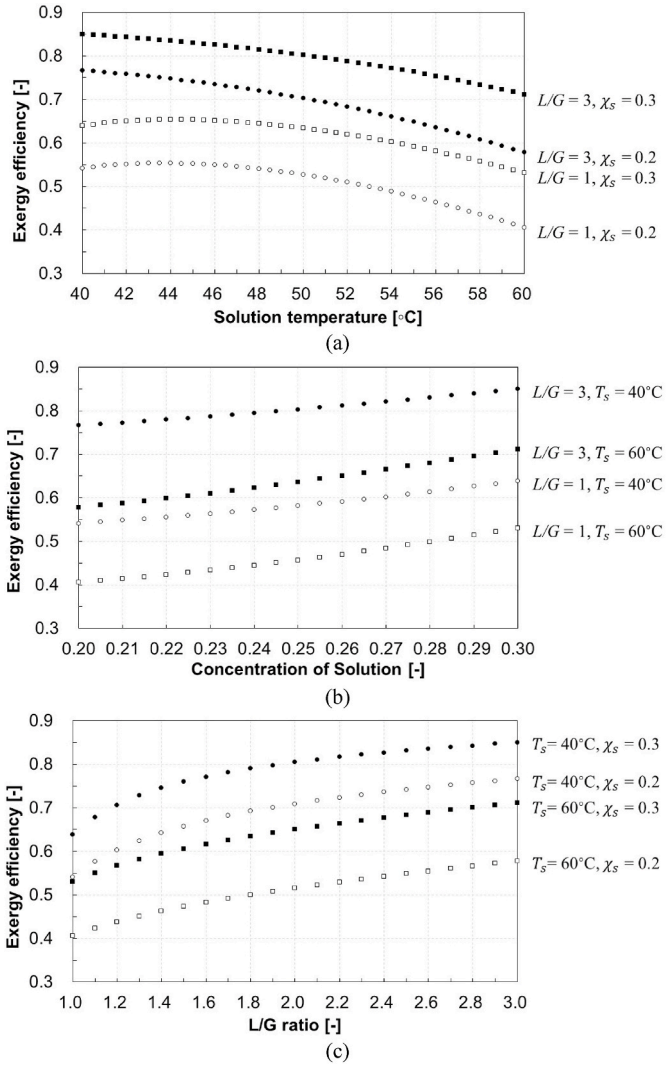

Fig. 10. Effects of operational parameters on the exergy efficiency during the humidification process.

partial vapor pressure of the desiccant solution increased. Simultaneously, the humidification performance increased. However, the exergy efficiency decreased, indicating that the rate of increase of exergy was higher than that of the effectiveness of the regenerator. In addition, the optimal temperature was 44 °C when the L/G was 1. However, the overall trend was that the lower the temperature of the desiccant solution, the higher the exergy efficiency.

4.4. Suitable operation of the regenerator for humidification

Based on the results from Sections 4.2 and 4.3, the suitable operation settings for the regenerator can be summarized as follows.

- A higher L/G is recommended to achieve higher COP and exergy efficiency.
- A lower concentration of desiccant solution is recommended for a higher COP, even though the exergy efficiency reduces with a lower concentration of desiccant solution.
- A higher temperature of the desiccant solution is recommended to achieve a higher COP; however, a lower temperature of the desiccant solution can be recommended to achieve a higher exergy efficiency for a sustainable system by reducing the energy losses.

The first point is apparent based on the analyzed results. Additionally, in the second point, the main factor in determining the concentration of the desiccant solution is the improvement of the humidification performance, because no energy is used to control the desiccant solution concentration. Therefore, a lower concentration is recommended, which results in a higher humidification performance.

The third point, regarding the temperature of the desiccant solution, was the main issue in many studies in which the regenerator was purposed to regenerate the desiccant solution in the cooling season. Similar to the results from this study, the humidification performance increased with the solution inlet temperature in previous studies [17,18,47,48] that investigated the humidification performance in the cooling season. In addition, Dong et al. [18] reported that the optimal solution temperature was 65 °C for regenerating the desiccant solution to achieve the best humidification performance with less energy consumption. Meanwhile, Guan et al. [49] found that a temperature between 40 and 50 °C is optimum considering exergy, and Naik et al. [46] reported that the exergy efficiency decreased with an increase in solution temperature.

Because the heat used in the regenerator is the major energy form used in the entire system, it is important to design the heat source and temperature of the desiccant solution at the regenerator. Therefore, the energy efficiency should be prioritized over the exergy efficiency in reducing the total energy consumption. However, a low exergy efficiency means that the potential of energy losses with irreversible reaction is increased; thus, the system requires further improvement for providing heat, such as more insulation. Moreover, a higher solution temperature requires a larger capacity for heating equipment and a higher insulation thermal storage tank.

Consequently, a lower solution temperature can be recommended, and the best strategy for the regenerator is to use the free heat from a low-temperature heat source, which is usually unusable and lost to the atmosphere or in liquid wastes [50]. During normal operation, a low inlet solution temperature can be used, and an auxiliary heater can be employed to increase the inlet solution temperature when further humidification is necessary.

5. Conclusions

Prediction models for the humidification performance of the LD system during the heating season were developed based on the performance data from a series of experiments. The humidification performance was quantified through the effectiveness results of regeneration and enthalpy exchange to predict the outlet state of the process air and desiccant solution. The heating and humidification performance of the regenerator was sufficient to satisfy indoor comfort in terms of temperature and humidity during the heating season.

From the correlation analysis, the L/G showed highly positive correlation coefficients of 0.898 and 0.890 with the regeneration and enthalpy exchange effectiveness, respectively. While, there were negative correlations between the temperature of desiccant solution with two effectiveness values (R = -0.342 and -0.372 for regeneration and enthalpy exchange effectiveness). In case of the concentration of desiccant solution, it was negatively correlated with the regeneration effectiveness (R = -0.054), however it has positive correlation with the enthalpy exchange effectiveness (R = 0.090). Based on the significantly correlated design parameters, two empirical models for regeneration and enthalpy exchange effectiveness were developed and showed good R^2 values over 0.92, and were verified within 10% of the RMSE from the additional experimental cases under the actual operations in the heating season. In addition, the prediction model for the Sherwood number was developed to numerically simulate the performance of regenerator during the heating season. It showed the 12% of RMSE compared with the actual humidification performance.

Using the developed models, the suitable operation settings for the regenerator were investigated considering the energy and exergy efficiencies. It was revealed that a high L/G is recommended to achieve both high energy and exergy efficiencies. In addition, a low concentration and high temperature of the desiccant solution resulted in a higher system COP. However, a lower solution temperature of 40 °C can be recommended as well as use of low-temperature heat from renewable energy sources and waste heat in buildings. In this study, the low solution temperature demonstrated higher exergy efficiency, indicating a more sustainable system, and reduced the potential for energy losses with irreversible reactions that degrade the system performance. Moreover, use of a low-temperature solution can reduce the size of the heating equipment and insulation of the thermal storage tank.

Thus, simplified models and suitable operation settings were considered for the humidification performance during the heating season for heating and humidifying the outdoor air. In future studies, the developed models will be applied to the HPLD-assisted air conditioning unit to improve the performance of the unit during the heating season. The heating and humidification cannot be controlled independently because of their interconnection; therefore, practical control logic will be established considering the indoor thermal comfort in the future. Furthermore, the suitable concentration of desiccant solution is necessary to be investigated considering the energy performance and freezing problem.

CRediT authorship contribution statement

Hansol Lim: Conceptualization, Methodology, Data curation, Writing – original draft. **Soo-Jin Lee:** Conceptualization, Data curation. **Yuehong Su:** Methodology, Writing – review & editing. **Jae-Weon Jeong:** Supervision, Validation, Writing – review & editing.

Declaration of competing interest

The authors declare that they have no known competing financial interests or personal relationships that could have appeared to influence the work reported in this paper.

Acknowledgment

This work was supported by the National Research Foundation of Korea (NRF) grants 2020R1A6A3A03037694 and 2019R1A2C2002514.

Appendix A. Experimental sets

Table A.1
Experimental sets for developing the empirical models to predict the humidification performance

Set	L/G [−]	χ_s [−]	T_s [°C]	T_a [°C]	ω_a [kg/kg$_a$]
1	1	0.2	40	8	0.004
2	1	0.2	60	8	0.004
3	1	0.3	40	8	0.004
4	1	0.3	60	8	0.004
5	1	0.2	40	12	0.007
6	1	0.2	60	12	0.007
7	1	0.3	40	12	0.007
8	1	0.3	60	12	0.007
9	1	0.2	40	16	0.006
10	1	0.2	60	16	0.006
11	1	0.3	40	16	0.006
12	1	0.3	60	16	0.006
13	1	0.2	40	20	0.010
14	1	0.2	60	20	0.010
15	1	0.3	40	20	0.010
16	1	0.3	60	20	0.010
17	2	0.2	40	8	0.004
18	2	0.2	60	8	0.004
19	2	0.3	40	8	0.004
20	2	0.3	60	8	0.004
21	2	0.2	40	12	0.007
22	2	0.2	60	12	0.007
23	2	0.3	40	12	0.007
24	2	0.3	60	12	0.007
25	2	0.2	40	16	0.006
26	2	0.2	60	16	0.006
27	2	0.3	40	16	0.006
28	2	0.3	60	16	0.006
29	2	0.2	40	20	0.010
30	2	0.2	60	20	0.010
31	2	0.3	40	20	0.010
32	2	0.3	60	20	0.010
33	3	0.2	40	8	0.004
34	3	0.2	60	8	0.004
35	3	0.3	40	8	0.004
36	3	0.3	60	8	0.004
37	3	0.2	40	12	0.007
38	3	0.2	60	12	0.007
39	3	0.3	40	12	0.007
40	3	0.3	60	12	0.007
41	3	0.2	40	16	0.006
42	3	0.2	60	16	0.006
43	3	0.3	40	16	0.006
44	3	0.3	60	16	0.006
45	3	0.2	40	20	0.010
46	3	0.2	60	20	0.010
47	3	0.3	40	20	0.010
48	3	0.3	60	20	0.010

Table A.2
Experimental sets for validating the developed empirical models for the humidification performance

Set	L/G [−]	χ_s [−]	T_s [°C]	Group
1	1	0.2	40	I
2	1	0.2	40	II
3	1	0.2	40	III
4	1	0.2	60	I
5	1	0.2	60	II
6	1	0.2	60	III
7	1	0.3	40	I
8	1	0.3	40	II
9	1	0.3	40	III
10	1	0.3	60	I
11	1	0.3	60	II
12	1	0.3	60	III
13	3	0.2	40	I
14	3	0.2	40	II
15	3	0.2	40	III
16	3	0.2	60	I

(*continued on next page*)

Table A.2 (*continued*)

Set	L/G [−]	χ_s [−]	T_s [°C]	Group
17	3	0.2	60	II
18	3	0.2	60	III
19	3	0.3	40	I
20	3	0.3	40	II
21	3	0.3	40	III
22	3	0.3	60	I
23	3	0.3	60	II
24	3	0.3	60	III

* Group I: Outdoor air temperature between -10 and -5 °C.
Group II: Outdoor air temperature between -5 and 0 °C.
Group III: Outdoor air temperature between 0 and 5 °C.

Appendix B. Numerical simulation models

The numerical method to simulate the humidification performance is described in this appendix. Two dimensional numerical simulation model was constructed based on the energy and mass balance equations [18,39] based on some assumptions as below.

- The analyzed system is adiabatic.
- The Lewis number is unity.
- The local heat and mass transfer coefficients are uniform for all positions of the regenerator.
- The surface area for heat and mass transfer is equal to the specific surface area of the honeycomb structure packing.
- It is negligible that the effects of diffusion, radiation, or radiation on the mass or heat transfer.

The directions for air flow and desiccant solution flow were defined in x-axis and y-axis in this study. The energy and mass conservation equations for each differential node in the regenerator are shown in Eqs. (B.1) to (B.3).

$$\frac{\dot{m}_a}{H}\frac{\partial \omega_a}{\partial x}+\frac{1}{L}\frac{\partial \dot{m}_s}{\partial y}=0 \tag{B.1}$$

$$\frac{\dot{m}_a}{H}\frac{\partial h_a}{\partial x}+\frac{1}{L}\frac{\partial\left(\dot{m}_s h_s\right)}{\partial y}=0 \tag{B.2}$$

$$\mathrm{d}\left(\dot{m}_s\%\chi_s\right)=0 \tag{B.3}$$

The overall mass and heat transfer between the air and desiccant solution are in Eqs. (B.4) to (B.6). The *Le* is usually assumed to be one, therefore Eq. (B.4) becomes Eq. (B.7). Additionally, the moisture transfers between the air and the desiccant solution can be defined in Eq. (B.8). The initial boundary conditions are expressed in Eq. (B.9). The mass transfer coefficient (h_m) can be derived using model for Sherwood number in Section 3.5 and the specifications of honeycomb structure packing are described in Section 2.2.

$$\frac{\partial h_a}{\partial x}=\frac{NTU_m Le}{L}\left[\left(h_{eq}-h_a\right)+\lambda_{T_s}\left(\frac{1}{Le}-1\right)\left(\omega_{eq}-\omega_a\right)\right] \tag{B.4}$$

$$NTU_m=\frac{h_m \alpha_s V}{\dot{m}_a} \tag{B.5}$$

$$Le=\frac{h}{h_m c_{p,a}} \tag{B.6}$$

$$\frac{\partial h_a}{\partial x}=\frac{NTU_m}{L}\left(h_{eq}-h_a\right) \tag{B.7}$$

$$\frac{\partial \omega_a}{\partial x}=\frac{NTU_m}{L}\left(\omega_{eq}-\omega_a\right) \tag{B.8}$$

$$\begin{aligned} &h_a=h_{a,\,i}, T_a=T_{a,\,i},\ \omega_a=\omega_{a,\,i}\ at\ x=0\\ &h_s=h_{s,\,i}, T_s=T_{s,\,i},\ \chi_s=\chi_{s,\,i}\quad at\ y=0 \end{aligned} \tag{B.9}$$

After discretization, the equations above are expressed in Eqs. (B.10) to (B.14). The mesh consists of M × N nodes, and the number of M and N was both 50. The number of nodes was selected which showed converged and stable results while increasing it from the low nodes. Therefore, the differential elements of *dx* and *dy* can be expressed as $\frac{L}{M}$ and $\frac{H}{N}$, respectively. The outlet air temperature can be calculated using the enthalpy and humidity ratio of air. In addition, the temperature of desiccant solution can be obtained from the enthalpy and concentration of desiccant solution based on the property of LiCl. Consequently, the regeneration and enthalpy exchange effectiveness can be obtained from the outlet condition of air and desiccant solution in the numerical simulation.

$$\dot{m}_a\left(\omega_a[i+1,\,j]-\omega_a[i,\,j]\right)=\frac{N}{M}\left(\dot{m}_s[i,j]-\dot{m}_s[i,j+1]\right) \tag{B.10}$$

$$\dot{m}_a(h_a[i+1,\ j]-h_a[i,\ j])=\frac{N}{M}\left(\dot{m}_s[i,j]\%h_s[i,\ j]-\dot{m}_s[i,j+1]\%h_s[i,\ j+1]\right) \tag{B.11}$$

$$\dot{m}_s[i,j+1]\%\chi_s[i,j+1]=\dot{m}_s[i,j]\%\chi_s[i,j] \tag{B.12}$$

$$\omega_a[i+1,j]-\omega_a[i,j]=\frac{NTU_m}{M}\left(\omega_{eq}[i,j]-\omega_a[i,j]\right) \tag{B.13}$$

$$h_a[i+1,j]-h_a[i,j]=\frac{NTU_m}{M}\left(h_{eq}[i,j]-h_a[i,j]\right) \tag{B.14}$$

References

[1] Policies database, Int. Energy Agency. https://www.iea.org/policies.
[2] K.E. Agency, Zero Energy Building Certification, 2020. https://zeb.energy.or.kr/.
[3] D. Aydin, S.P. Casey, X. Chen, S. Riffat, Numerical and experimental analysis of a novel heat pump driven sorption storage heater, Appl. Energy 211 (2018) 954–974, https://doi.org/10.1016/j.apenergy.2017.11.102.
[4] The Future of Cooling, Opportunities for Energy-Efficient Air-Conditioning, Int. Energy Agency., 2018, https://doi.org/10.1787/9789264301993-en.
[5] D. D'Agostino, L. Mazzarella, What is a Nearly zero energy building? Overview, implementation and comparison of definitions, J. Build. Eng. 21 (2019) 200–212, https://doi.org/10.1016/j.jobe.2018.10.019.
[6] W. Wu, H.M. Skye, Net-zero nation: HVAC and PV systems for residential net-zero energy buildings across the United States, Energy Convers. Manag. 177 (2018) 605–628, https://doi.org/10.1016/j.enconman.2018.09.084.
[7] A. Gurubalan, M.P. Maiya, P.J. Geoghegan, A comprehensive review of liquid desiccant air conditioning system, Appl. Energy 254 (2019) 113673, https://doi.org/10.1016/j.apenergy.2019.113673.
[8] C.E.L. Nobrega, N.C.L. Brum, Desiccant-Assisted Cooling: Fundamentals and Applications, Springer, 2014, https://doi.org/10.1007/978-1-4471-5565-2.
[9] T. Zhang, X. Liu, Y. Jiang, Performance optimization of heat pump driven liquid desiccant dehumidification systems, Energy Build. 52 (2012) 132–144, https://doi.org/10.1016/j.enbuild.2012.06.002.
[10] Y. Xie, T. Zhang, X. Liu, Performance investigation of a counter-flow heat pump driven liquid desiccant dehumidification system, Energy 115 (2016) 446–457, https://doi.org/10.1016/j.energy.2016.09.037.
[11] H. Lim, J.W. Jeong, Energy saving potential of thermoelectric modules integrated into liquid desiccant system for solution heating and cooling, Appl. Therm. Eng. 136 (2018) 49–62, https://doi.org/10.1016/j.applthermaleng.2018.02.096.
[12] W. Su, X. Zhang, Performance analysis of a novel frost-free air-source heat pump with integrated membrane-based liquid desiccant dehumidification and humidification, Energy Build. 145 (2017) 293–303, https://doi.org/10.1016/j.enbuild.2017.04.024.
[13] J.H. Lee, J.Y. Ko, J.W. Jeong, Design of heat pump-driven liquid desiccant air conditioning systems for residential building, Appl. Therm. Eng. 183 (2021) 116207, https://doi.org/10.1016/j.applthermaleng.2020.116207.
[14] S.J. Lee, H. Lim, J.W. Jeong, Energy benefit of liquid desiccant-assisted humidification in buildings during winter operation, Energies 14 (2021) 1360, https://doi.org/10.3390/en14051360.
[15] P. Gandhidasan, Quick performance prediction of liquid desiccant regeneration in a packed bed, Sol. Energy 79 (2005) 47–55, https://doi.org/10.1016/j.solener.2004.10.002.
[16] Y. Luo, H. Yang, L. Lu, R. Qi, A review of the mathematical models for predicting the heat and mass transfer process in the liquid desiccant dehumidifier, Renew. Sustain. Energy Rev. 31 (2014) 587–599, https://doi.org/10.1016/j.rser.2013.12.009.
[17] M.H. Kim, J.Y. Park, J.W. Jeong, Simplified model for packed-bed tower regenerator in a liquid desiccant system, Appl. Therm. Eng. 89 (2015) 717–726, https://doi.org/10.1016/j.applthermaleng.2015.06.057.
[18] H.W. Dong, H.J. Cho, J.Y. Park, J.W. Jeong, Optimum regeneration temperature of a desiccant solution in a packaged liquid desiccant-assisted air conditioning unit, Int. J. Refrig. 101 (2019) 155–166, https://doi.org/10.1016/j.ijrefrig.2019.03.037.
[19] V. Martin, D.Y. Goswami, Effectiveness of heat and mass transfer processes in a packed bed liquid desiccant dehumidifier/regenerator, HVAC R Res. 6 (2000) 21–39.
[20] G.I. Sultan, A.M. Hamed, A.A. Sultan, The effect of inlet parameters on the performance of packed tower-regenerator, Renew. Energy 26 (2002) 271–283, https://doi.org/10.1016/S0960-1481(01)00113-6.
[21] W. Tao, L. Yimo, L. Lin, A novel 3D simulation model for investigating liquid desiccant dehumidification performance based on CFD technology, Appl. Energy 240 (2019) 486–498, https://doi.org/10.1016/j.apenergy.2019.02.068.
[22] X. Guo, T. Wen, M. Wang, Y. Luo, X. She, Performance investigation of a liquid desiccant regenerator with CFD technology, Appl. Therm. Eng. 184 (2021) 116055, https://doi.org/10.1016/j.applthermaleng.2020.116055.
[23] X. Wang, W. Cai, J. Lu, Y. Sun, X. Ding, Heat and mass transfer model for desiccant solution regeneration process in liquid desiccant dehumidification system, Ind. Eng. Chem. Res. 53 (2014) 2820–2829, https://doi.org/10.1021/ie403102x.
[24] P. Mecenas, R.T. da Rosa Moreira Bastos, A.C. Rosário Vallinoto, D. Normando, Effects of temperature and humidity on the spread of COVID-19: a systematic review, PLoS One 15 (2020) 1–21, https://doi.org/10.1371/journal.pone.0238339.
[25] J. Wang, K. Tang, K. Feng, X. Lin, W. Lv, K. Chen, F. Wang, High Temperature and High Humidity Reduce the Transmission of COVID-10, ArXiv Prepr. Arxiv, 2020.
[26] J.H. Shin, J.Y. Park, M.S. Jo, J.W. Jeong, Impact of heat pump-driven liquid desiccant dehumidification on the energy performance of an evaporative cooling-assisted air conditioning system, Energies 11 (2018) 345, https://doi.org/10.3390/en11020345.
[27] J.Y. Park, Dehumidification Performance Control for Cooling Energy Conservation in a Packaged Liquid Desiccant and Evaporative Cooling-Assisted Air Conditioning System, Hanyang University, 2019.
[28] Munters, CELdek Evaporative Media.
[29] Technical data Sheet for UP500, Hyubshin.
[30] ASHRAE, International Weather for Energy Calculations, 2011. Version 2.
[31] M.R. Conde, Properties of aqueous solutions of lithium and calcium chlorides: formulations for use in air conditioning equipment design, Int. J. Therm. Sci. 43 (2004) 367–382, https://doi.org/10.1016/j.ijthermalsci.2003.09.003.
[32] Stat-Ease, Design Expert® Version 11 Software, 2018.
[33] ASHRAE Guideline 2-2010: Engineering Analysis of Experimental Data, 2010.
[34] ASHRAE Handbook: HVAC systems and Equipment, Chapter 22: Humidifier, 2020, https://doi.org/10.1097/JDN.0000000000000436.
[35] ANSI/ASHRAE Standard 55-2013: Thermal Environmental Conditions for Human Occupancy, 2013.
[36] T.W. Chung, H. Wu, Comparison between spray towers with and without fin coils for air dehumidification using triethylene glycol solutions and development of the mass-transfer correlations, Ind. Eng. Chem. Res. 39 (2000) 2076–2084, https://doi.org/10.1021/ie990630d.
[37] M. Meyer, M. Hendou, M. Prevost, Simultaneous heat and mass transfer model for spray tower design: application on VOCs removal, Comput. Chem. Eng. 19 (1995) 277–282, https://doi.org/10.1016/0098-1354(95)87049-0.
[38] S. V Potnis, T.G. Lenz, Dimensionless mass-transfer correlations for packed-bed liquid-desiccant contactors, Ind. Eng. Chem. Res. 35 (1996) 4185–4193.
[39] X.H. Liu, Y. Jiang, K.Y. Qu, Heat and mass transfer model of cross flow liquid desiccant air dehumidifier/regenerator, Energy Convers. Manag. 48 (2007) 546–554, https://doi.org/10.1016/j.enconman.2006.06.002.
[40] ASHRAE Handbook Fundamentals, Chapter14: Climatic Design Information, 2013.
[41] M.H. Kim, J.H. Hwang, Performance prediction of a hybrid ventilation system in an apartment house, Energy Build. 41 (2009) 579–586, https://doi.org/10.1016/j.enbuild.2008.12.003.
[42] H. Lim, J.W. Jeong, Energy saving potential of thermoelectric radiant cooling panels with a dedicated outdoor air system, Energy Build. 169 (2018) 353–365, https://doi.org/10.1016/j.enbuild.2018.03.062.
[43] M.H. Kim, S.W. Ham, J.S. Park, J.W. Jeong, Impact of integrated hot water cooling and desiccant-assisted evaporative cooling systems on energy savings in a data center, Energy 78 (2014) 384–396, https://doi.org/10.1016/j.energy.2014.10.023.
[44] H. Lim, J.W. Jeong, Thermoelectric module integrated fuel cell in a liquid desiccant-assisted air-conditioning system, Heat Tran. Eng. 41 (2020) 779–799, https://doi.org/10.1080/01457632.2019.1576412.
[45] I. Dincer, A. Abu-rayash, Chapter 6. Sustainability modeling, in: Energy Sustain., first ed., Elsevier, 2020.
[46] B.K. Naik, P. Muthukumar, Energy, entransy and exergy analyses of a liquid desiccant regenerator, Int. J. Refrig. 105 (2019) 80–91, https://doi.org/10.1016/j.ijrefrig.2018.08.016.
[47] Y. Yin, X. Zhang, Z. Chen, Experimental study on dehumidifier and regenerator of liquid desiccant cooling air conditioning system, Build. Environ. 42 (2007) 2505–2511, https://doi.org/10.1016/j.buildenv.2006.07.009.
[48] M.M. Bassuoni, An experimental study of structured packing dehumidifier/regenerator operating with liquid desiccant, Energy 36 (2011) 2628–2638, https://doi.org/10.1016/j.energy.2011.02.004.
[49] B. Guan, X. Liu, T. Zhang, Analytical solutions for the optimal cooling and heating source temperatures in liquid desiccant air-conditioning system based on exergy analysis, Energy 203 (2020) 117860, https://doi.org/10.1016/j.energy.2020.117860.
[50] P. Luis, Chapter 8 - hybrid processes based on membrane technology, in: Fundam. Model. Membr. Syst. Membr. Process Perform., first ed., Elsevier, Washington, D. C., 2018 https://doi.org/10.1016/C2016-0-02489-0.